Thermal Impedance and Gain Switching of 1550 nm Room Temperature Continuous-wave Electrically Pumped Laser Diode Monolithically Grown on Silicon

Bei Shi[1], Sergio Pinna[1], Bowen Song[1], Hongwei Zhao[1], and Jonathan Klamkin[1]
[1]*Electrical and Computer Engineering Department, University of California, Santa Barbara, CA 93106, USA*
E-mail: beishi@ucsb.edu

Abstract: A room-temperature continuous-wave electrically pumped quantum well laser was realized on on-axis (001) silicon. Measurements demonstrated lasing up to 65°C, a thermal impedance of 8.1°C/W, and a narrow gain-switched optical pulse width of 1.5 ns.
OCIS codes: (130.3120) Integrated optics devices; (140.5960) Semiconductor lasers; (250.5300) Photonic integrated circuits

1. Introduction

Silicon photonics (SiPh) is recognized as a strategic technology solution to address the growing data center market and global IP traffic [1]. An on-chip light source is a critical building block for SiPh to enable large-scale integration. SiPh leverages complementary metal-oxide-semiconductor (CMOS) processes, and laser integration relies on the integration of III-V materials on silicon (Si). Monolithic integration via heteroepitaxy is most appealing for achieving low-cost and high-volume production that would avoid precision assembly processes. The challenges to be resolved for III-V on Si heteroepitaxy are primarily associated with generation of crystalline defects and efficient coupling to Si-based waveguides. Recent progress in direct epitaxy of 1310 nm indium arsenide (InAs) quantum dot (QD) lasers on Si have demonstrated promise for optical interconnects in data centers [2]. Further exploration of 1550 nm lasers on Si could advance free-space and long-haul communications, as well as LIDAR applications, but extending to this wavelength region is challenging. In this work, we report the realization of a continuous-wave (CW) electrically pumped diode laser on Si using an indium phosphide (InP) metamorphic buffer grown by metalorganic chemical vapor deposition (MOCVD). Owing to a low dislocation density InP buffer (1.15×10^{8} cm^{-2}), a seven-layer quantum well (QW) laser was realized and operates CW up to 65°C, and under pulsed conditions to greater than 105°C. Additionally, thermal impedance and gain switching experiments were performed on these Si-based lasers, for the first time. Experimental results have revealed a low thermal impedance of 8.1°C/W, only slightly higher than that demonstrated on native InP with identical device geometries. Compressed pulse durations were achieved as short as 1.5 ns under direct modulation, driven by electrical pulses with a width of 12.5 ns. The results represent a significant advancement toward fully monolithic 1550 nm lasers on Si.

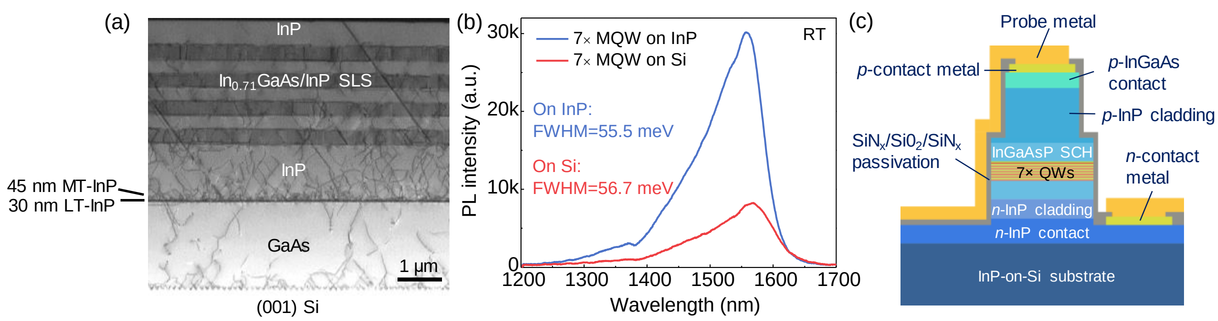

Fig. 1. (a) Cross-sectional STEM of the 3.9 µm InP grown on V-grooved (001) Si. (b) Low power excitation RT-PL spectra of seven-layer InGaAsP based QWs grown on InP-on-Si template and InP native substrate. (c) Schematic diagram of the InP laser diode on (001) Si.

2. Device implementation and lasing characteristics

The material growth, including the InP-on-Si template and the seven-layer QW laser structure, was completed using a horizontal low-pressure MOCVD system. For the InP-on-Si template, a gallium arsenide (GaAs)-on-V-grooved Si (GoVS) template was first grown to eliminate anti-phase boundaries (APBs), and to gradually alleviate the lattice mismtach between InP and Si (~8%) [3]. Subsequently, a three-step InP buffer was grown to achieve a smooth surface and a low defect density. Further defect mitigation was enabled by inserting four periods of 13 nm $In_{0.71}Ga_{0.29}As$/19 nm InP strained layer superlattices (SLSs). Figure 1(a) presents the cross-sectional scanning transmission electron microscopy (STEM) image of the InP-on-Si template. The majority of threading dislocations

(TDs) are bent and filtered by the SLSs. Room temperature photoluminescence (RT-PL) spectra shown in Fig. 1(b) reveal a comparable intensity and full-width half-maximum (FWHM) for the InGaAsP based QWs on InP and on Si.

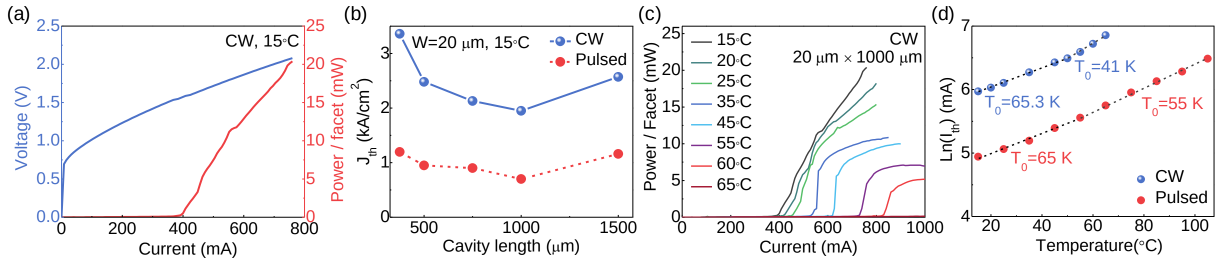

Fig. 2. (a) LIV characteristics of a 20×1000 μm^2 laser on Si measured at 15ºC. (b) Dependence of lasing threshold current density on cavity length under CW and pulsed operation. (c) CW LI characteristics for the 20×1000 μm^2 ridge laser on Si as a function of stage temperature. (d) Temperature dependence of threshold current under CW and pulsed operation.

Following growth, the as-grown sample was fabricated into ridge waveguide Fabry-Perot (FP) laser bars, which were mounted onto ceramic carriers for subsequent characterization. Figure 2(a) shows the light-current-voltage (LIV) characteristics of a 20×1000 μm^2 device. CW operation with a threshold current density (J_{th}) of 1.95 kA/cm^2 was demonstrated, with the maximum single facet output power reaching 20 mW. The wall-plug efficiency (WPE) was calculated to be 2.7%. As a reference, devices with the same geometry were fabricated on InP substrates, yielding a lower J_{th} of 0.65 kA/cm^2, together with a higher WPE of 15%. The series resistance for the laser on Si was measured to be approximately 1.7 Ω, which is more than twice that for the laser on InP (0.8 Ω). The dependence of J_{th} on the laser cavity length is illustrated in Fig. 2(b), where the J_{th} is generally lower for longer cavity lengths. It is observed that under pulsed operation (300 ns pulse width, 10% duty cycle), the J_{th} is approximately half of the value under CW operation, which is ascribed to device self-heating. The self-heating originates from a much thinner *n*-doped InP layer on Si and subsequent higher series resistance, as well as a lower injection efficiency due to the relatively high density of defects shown in Fig. 1(a). Despite these shortcomings, the devices operate CW up to 65°C, as shown in Fig. 2(c). The highest output power per facet is 5 mW at 60°C. From Fig. 2(d) the characteristic temperatures (T_0) under both CW and pulsed operation were extracted, where a lower T_0 value was identified between 40°C and 65°C for CW. In contrast, the threshold temperature stability is apparently improved on InP, and its highest CW operation temperature is 95°C. These comprehensive comparisons suggest the influence of dislocations generated from the III-V/Si interface on the lasing characteristics, providing valuable insight for further improving the material quality and ultimately improving device performance.

3. Thermal impedance measurements

In addition to the fundamental LIV characterization, the lasing spectra were also measured at various operating temperatures and current levels. As shown in Fig. 3(a), an apparent red-shift was observed when the stage temperature was increased by 10°C. It would therefore be informative to quantify the thermal impedance for both lasers on Si and on InP. The extraction of thermal impedance (Z_T) follows the methodology described in [4]. By combining the power- and temperature-dependent FP mode wavelength shifts for CW and pulsed operation, respectively, the Z_T value can be obtained from: $Z_T = (\Delta\lambda/\Delta P)/(\Delta\lambda/\Delta T)$. Results demonstrate that the 20×500 μm^2 laser on Si yields a thermal impedance of 8.1°C/W, whereas the Z_T value for the laser on InP with an identical geometry is slightly lower, 5.7°C/W. Considering that Si is more thermally conductive compared to InP, the higher thermal impedance for the laser on Si may be attributed to the more severe device heating discussed earlier. This could arise from the residual thermal strain in the InP template and the defective InP/GaAs and GaAs/Si interfaces.

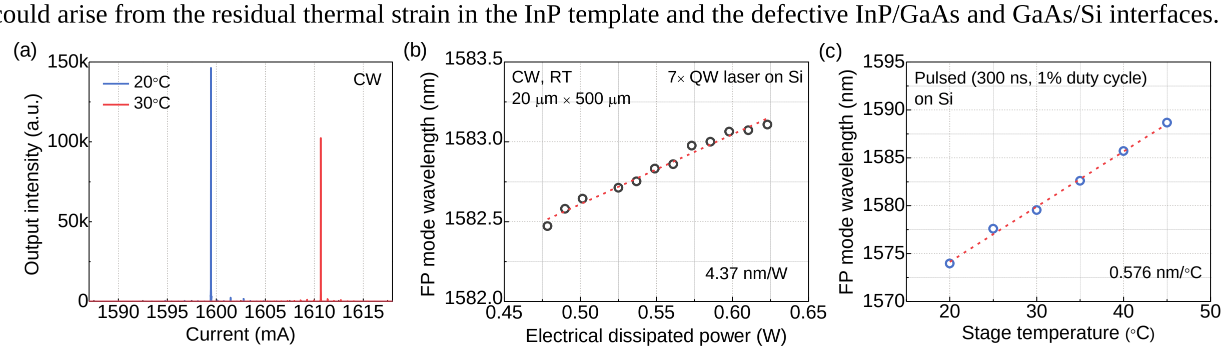

Fig. 3. (a) Lasing spectra for a 20×500 μm^2 device on Si at 20ºC and 30ºC, respectively. (b) CW FP mode wavelength shift as a function of dissipated electrical power. (c) Pulsed FP mode wavelength shift as a function of stage temperature.

4. Gain-switching of 1550 nm laser epitaxially grown on Si

Of growing interest since the 1990s is the investigation of gain-switched semiconductor laser diodes for generating ultrashort pulses as narrow as a few nanoseconds or tens and hundreds of picoseconds with reasonable output power [5]. To investigate such concepts for the InP laser on Si, electrical pulses were applied with widths ranging from 7.25 ns to 50 ns. These were superimposed onto a direct current (DC) bias of 100 mA to drive the 10×500 μm^2 laser on Si. The output optical pulse was amplified and measured by an oscilloscope in the time domain. Figure 4 (a) presents results on the compression of the input pulse at various driving current levels. It is observed that the optical pulse is more compressed by narrower electrical pulses. For example, as shown in the magnified diagram in the inset of Fig. 4(a), driven by an electrical pulse with a current amplitude of 135 mA and a duration of 12.5 ns, the gain-switched optical pulse width is as narrow as 1.5 ns. However, a too narrow electrical pulse would inversely broaden the optical pulse due to insufficient carriers to switch the laser on, while a long driving pulse also results in the broadening of gain-switched pulses [6]. On the other hand, Fig. 4(b) reveals that increasing the current amplitude first causes the optical pulse width to decrease, until a second relaxation appears [5], then subsequently increase due to excessive carrier injection. An example of an optical pulse observed on the oscilloscope is demonstrated in Fig. 4(c), demonstrating a pulse width of 1.8 ns. From a Gaussian simulation we extract the symmetric rise time (τ_R) of 1.3 ns and fall time (τ_F) of 1.4 ns. As discussed in [6], a low modal gain and high gain compression factor (ε) limit the optical pulse width. A similar gain-switched optical pulse width was measured for the identical device on InP. Although these results are promising, it is more appealing to apply this technique to single-mode lasers, such as distributed feedback lasers, to achieve ultrashort single-frequency pulses.

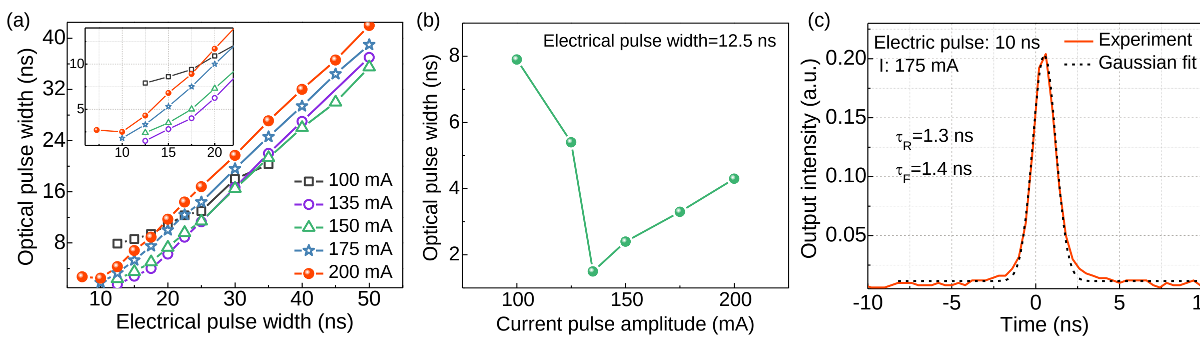

Fig. 4. (a) Optical pulse width versus electrical pulse width at various current amplitudes. The inset shows a magnified diagram for the short electrical pulse regime. (b) Optical pulse width versus current pulse amplitude for an electrical pulse width of 12.5 ns. (c) A gain-switched pulse from the Si-based laser diode with a driving current of 175 mA. Black dashed line represents a Gaussian fit.

5. Conclusion

In this paper, a 1550 nm CW electrically pumped laser diode was monolithically grown on (001) Si, demonstrating a reasonable lasing threshold current density of 1.95 kA/cm^2, a high output power of 20 mW per facet, and the capability of operating up to 65°C. The thermal impedance of the laser on Si was measured to be 8.1°C/W, which is slightly larger than the value obtained on native InP. Furthermore, a gain-switching experiment was performed, demonstrating an apparent compression of the optical pulses to as narrow as 1.5 ns. These results represent a major step towards high performance lasers integrated on the SiPh platform. Further experiments will be focused on producing single mode Si-based lasers and improving the III-V buffer quality.

Acknowledgements

The authors acknowledge funding from DARPA through the Young Faculty Award program and AIM Photonics.

References

[1] A. Castellano et al., "Room-temperature continuous-wave operation in the telecom wavelength range of GaSb-based lasers monolithically grown on Si," APL Photon. **2,** 061301 (2017).
[2] S. Liu et al., "High-channel-count 20 GHz passively mode-locked quantum dot laser directly grown on Si with 4.1 Tbit/s transmission capacity," Optica **6,** 128-134 (2019).
[3] B. Shi et al., "MOCVD grown low dislocation density GaAs-on-V-groove patterned (001) Si for 1.3 µm quantum dot laser applications," Appl. Phys. Lett. **114,** 172102 (2019).
[4] B. Song et al., "High-thermal performance 3D hybrid silicon lasers," IEEE Photon. Tech. Lett. **29,** 1143-1146 (2017).
[5] P. P Vasil'ev et al., "Fast phenomena in semiconductor lasers," Rep. Prog. Phys. **63,** 1997-2042 (2000).
[6] C. Hantschmann et al., "Gain switching of monolithic 1.3 µm InAs/GaAs quantum dot lasers on silicon," J. Lightwave Tech. **36,** 3837-3842 (2018).